Predicted image quality of a CMOS APS X-ray detector across a range of mammographic beam qualities

A Konstantinidis[1]
[1]Diagnostic Radiology and Radiation Protection, Christie Medical Physics and Engineering, The Christie NHS Foundation Trust, Manchester M20 4BX, UK

E-mail: Anastasios.Konstantinidis@christie.nhs.uk

Abstract. Digital X-ray detectors based on Complementary Metal-Oxide-Semiconductor (CMOS) Active Pixel Sensor (APS) technology have been introduced in the early 2000s in medical imaging applications. In a previous study the X-ray performance (i.e. presampling Modulation Transfer Function (pMTF), Normalized Noise Power Spectrum (NNPS), Signal-to-Noise Ratio (SNR) and Detective Quantum Efficiency (DQE)) of the Dexela 2923MAM CMOS APS X-ray detector was evaluated within the mammographic energy range using monochromatic synchrotron radiation (i.e. 17-35 keV). In this study image simulation was used to predict how the mammographic beam quality affects image quality. In particular, the experimentally measured monochromatic pMTF, NNPS and SNR parameters were combined with various mammographic spectral shapes (i.e. Molybdenum/Molybdenum (Mo/Mo), Rhodium/Rhodium (Rh/Rh), Tungsten/Aluminium (W/Al) and Tungsten/Rhodium (W/Rh) anode/filtration combinations at 28 kV). The image quality was measured in terms of Contrast-to-Noise Ratio (CNR) using a synthetic breast phantom (4 cm thick with 50% glandularity). The results can be used to optimize the imaging conditions in order to minimize patient's Mean Glandular Dose (MGD).

1. Introduction

Recently developed digital X-ray detectors based on Complementary Metal-Oxide-Semiconductor (CMOS) Active Pixel Sensor (APS) technology demonstrate higher performance compared to Charge-Coupled Device (CCD) and Thin Film Transistor (TFT) digital detectors. In a previous study [1] the X-ray performance of a CMOS APS X-ray detector (named Dexela 2923MAM) was experimentally evaluated within the mammographic energy range using monochromatic synchrotron radiation. In particular, the monochromatic presampling Modulation Transfer Function (pMTF), Normalized Noise Power Spectrum (NNPS), Signal-to-Noise Ratio (SNR) and Detective Quantum Efficiency (DQE) parameters were calculated for 17, 20, 23, 26, 29, 33, 33.3 and 35 keV. In the same study it was demonstrated that the monochromatic pMTF, NNPS and SNR data can be combined with different mammographic spectral shapes to predict the X-ray performance of the detector for any mammographic beam quality within the investigated energy range [1]. In the current work the monochromatic pMTF, NNPS and SNR parameters were combined with four X-ray spectral shapes. The resultant polychromatic data were inserted into an image simulation algorithm [2] to predict the respective mammographic image quality for given breast and exposure conditions.

2. Materials and Methods

Four radiation beam qualities (Molybdenum/Molybdenum (Mo/Mo), Rhodium/Rhodium (Rh/Rh), Tungsten/Rhodium (W/Rh) and Tungsten/Aluminium (W/Al) at 28 kV) were generated (using Boone's interpolating polynomial algorithm [3]) based on the IEC 62220-1-2 standard [4]. All X-ray spectra were attenuated by a synthetic average breast phantom (4 cm thick with 50% glandularity, including a cylindrical microcalcification (μC) with 600 μm diameter and 600 μm thickness). The parameters related to the attenuated X-ray spectra are shown in table 1. The used mammographic beam qualities were similar to the IEC ones (based on the Half Value Layer (HVL) values).

Table 1. Parameters related to the used radiation beam qualities for 28 kV tube voltage and 4 cm breast with 50% glandularity

Parameter	Mo/Mo	Rh/Rh	W/Rh	W/Al	Units
Anode	Mo	Rh	W	W	
Filtration	0.032 Mo	0.025 Rh	0.050 Rh	0.500 Al	mm
E_{mean}	19.4	20.9	20.9	22.2	keV
HVL	0.58	0.76	0.77	0.86	mm Al
IEC HVL	0.60	0.74	0.75	0.83	mm Al
Φ/Ka	5451	6251	6231	7087	(X-rays/mm^2/μGy)
Nom. Contrast	0.65	0.57	0.56	0.51	

Figure 1 shows the normalized spectral shapes (attenuated from the breast). Mo/Mo spectrum corresponds to lower energies, Rh/Rh and W/Rh to medium and W/Al to higher ones.

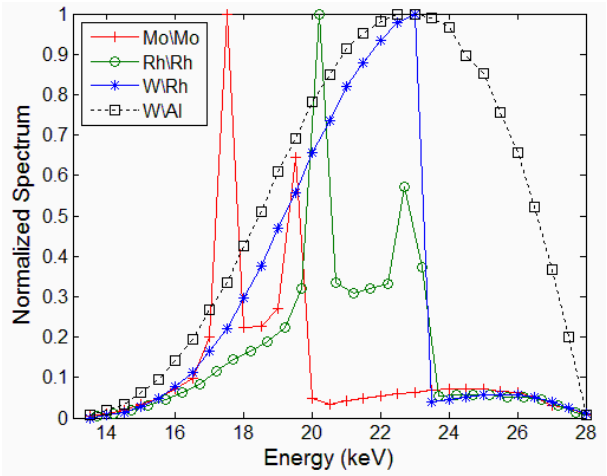

Figure 1. Normalized X-ray spectra for the used radiation beam qualities

These spectral shapes were used to calculate the polychromatic pMTF, NNPS and SNR values which were inserted in an image simulation algorithm [2] to add blurring, sampling and noise to ideal images of μC and surrounding breast tissue (with perfect uniformity). The Contrast-to-Noise Ratio (CNR) was calculated from the synthetic breast images. Figure 2 shows an ideal X-ray image, while Figure 3 shows the respective simulated one.

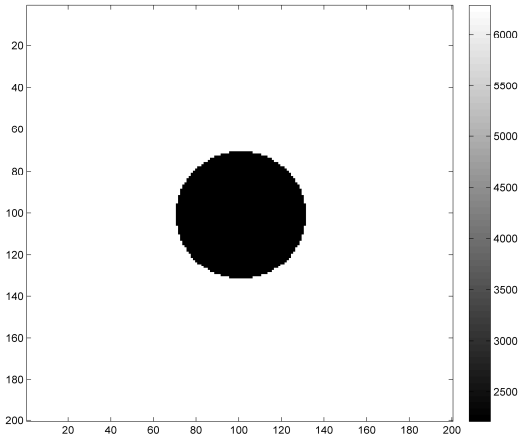

Figure 2. Ideal μC for 28 kV Mo/Mo (input)

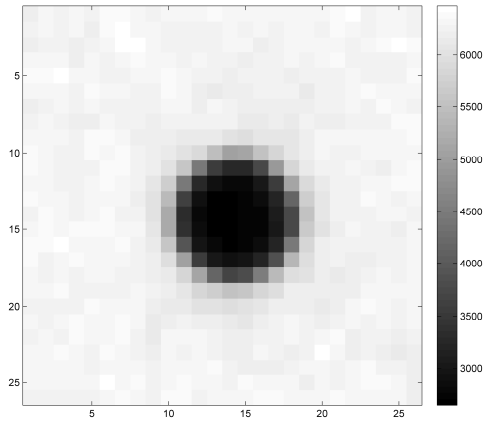

Figure 3. Simulated μC for 28 kV Mo/Mo

3. Results and Discussion

3.1. Simulation results for 3 mGy ESAK

Figure 4 shows the predicted polychromatic DQE values for 3 mGy Entrance Surface Air Kerma (ESAK), i.e. the radiation exposure at the breast entrance. Figure 5 depicts the respective CNR values. W/Rh spectrum shows the highest DQE and CNR values at the expense of high Mean Glandular Dose (MGD; see table 2), which was calculated based on [5]. This happens from the combination of the W/Rh spectral shape and the monochromatic energy deposition in the breast tissue (see [5]). On the other hand, Mo/Mo results in low Air Kerma at Detector surface (DAK), DQE and CNR values due to high attenuation from the breast. However, it demonstrates the lowest MGD value because most of the absorbed X-rays deposit their energy in the skin [5]. Finally, Rh/Rh and W/Al show similar CNR values although Rh/Rh has higher nominal contrast (see table 1) and DQE values. This probably happens because the X-ray sensitivity of the detector is higher for W/Al spectrum, resulting in improved statistics and higher SNR.

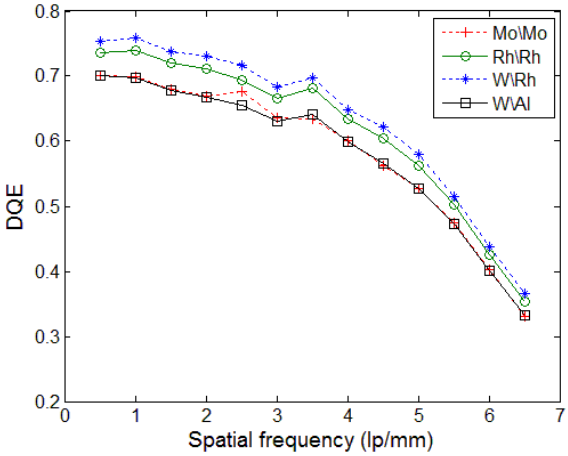

Figure 4. Predicted DQE for 3 mGy ESAK

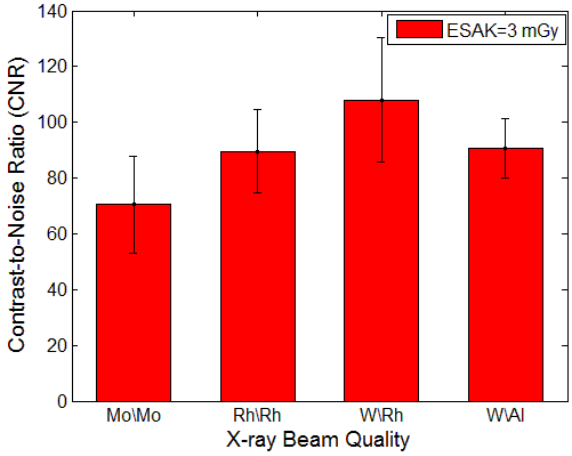

Figure 5. Predicted CNR for 3 mGy ESAK

Table 2. Calculated MGD and DAK for 3 mGy ESAK (4 cm breast with 50% glandularity)

Parameter	Mo/Mo	Rh/Rh	W/Rh	W/Al	Units
MGD	0.58	0.72	0.93	0.71	mGy
DAK	81.0	141.1	184.8	158.7	μGy

3.2.Simulation results for 100 μGy DAK

The predicted polychromatic DQE (figure 6) and CNR (figure 7) values were also calculated for an average mammographic DAK level, i.e. 100 μGy. In this case, Mo/Mo, Rh/Rh and W/Rh spectra result in high DQE values. In particular, the Mo/Mo spectrum corresponds to the highest CNR value, probably due to high nominal contrast (table 1). However, to reach 100 μGy DAK with Mo/Mo we need high ESAK (3.71 mGy) which results in high MGD (0.72 mGy) - see table 3. On the other hand, W/Rh results in high CNR and low MGD (0.5 mGy) because it requires low ESAK (1.62 mGy). It should be mentioned that the difference between the CNR values was within 13%.

Table 3. Calculated ESAK and MGD for 100 μGy DAK (4 cm breast with 50% glandularity)

Parameter	Mo/Mo	Rh/Rh	W/Rh	W/Al	Units
ESAK	3.71	2.13	1.62	1.89	mGy
MGD	0.72	0.51	0.5	0.45	mGy

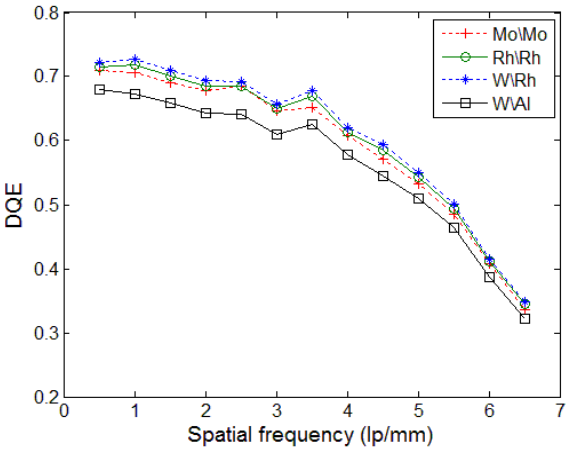

Figure 6. Predicted DQE for 100 μGy DAK

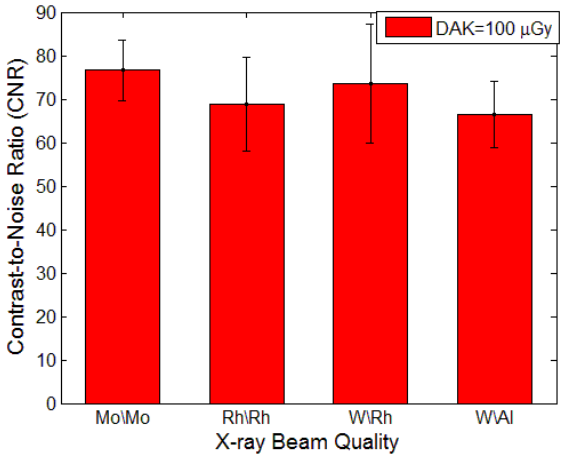

Figure 7. Predicted CNR for 100 μGy DAK

4. Conclusions and Future Work

This work demonstrates how the spectral shape affects the mammographic image quality (in terms of CNR) of a CMOS APS X-ray detector for given ESAK and DAK values. For a typical ESAK value (3 mGy) it was found that the W/Rh beam quality delivers the highest image quality at the expense of high MGD. Both Rh/Rh and W/Al spectra may deliver sufficient beam quality with lower MGD. For 100 μGy DAK the W/Rh spectrum delivers high CNR with low MGD. Further investigation needs to be made to optimize the image quality for low MGD. For example, various imaging conditions can be tested to deliver CNR values within a given range. Different X-ray spectra will be tested for various breast thickness (2-8 cm) and glandularity (0-100%) combinations. Finally, realistic software breast phantoms [6] and simulated scatter radiation effect [7] will be used to improve the simulation.

References

[1] Konstantinidis A C *et al* 2013 X-ray Performance Evaluation of the Dexela CMOS APS X-ray Detector Using Monochromatic Synchrotron Radiation in the Mammographic Energy Range *IEEE Transactions on Nuclear Science* 60 pp 3969–80

[2] Konstantinidis A C 2011 *Evaluation of digital X-ray detectors for medical imaging applications* (London: University College London)

[3] Boone J M, Fewell T R and Jennings R J 1997 Molybdenum, rhodium, and tungsten anode spectral models using interpolating polynomials with application to mammography *Medical Physics* vol 24 pp 1863–1874

[4] IEC 62220-1-2 2005 *Medical Electrical Equipment-Characteristics of Digital X-Ray Imaging Devices-Part 1-2: Determination of the Detective Quantum Efficiency-Mammography Detectors* (Geneva: International Electrotechnical Commission)

[5] Boone J M 2002 Normalized glandular dose (DgN) coefficients for arbitrary x-ray spectra in mammography: Computer-fit values of Monte Carlo derived data *Med. Phys.* 29 pp 869–874

[6] Bliznakova K, Sechopoulos I, Buliev I and Pallikarakis N 2012 BreastSimulator: A software platform for breast x-ray imaging research *Journal of Biomed. Graphics and Comp.* 2 pp 1–13

[7] Diaz O, Dance D R, Young K C, Elangovan P, Bakic P R and Wells K 2015 Estimation of scattered radiation in digital breast tomosynthesis *Phys. in Med. and Biol.* vol 59 pp 4375–4393